

# Multidimensional Protein Identification Technology-Selected Reaction Monitoring Improving Detection and Quantification for Protein Biomarker Studies

Christoph Krisp,<sup>†,‡</sup> Matthew J. McKay,<sup>†,§</sup> Dirk A. Wolters,<sup>‡</sup> and Mark P. Molloy<sup>\*,†,§</sup>

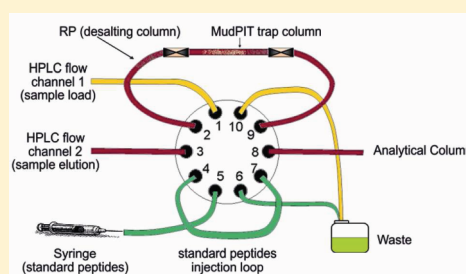
<sup>†</sup>Department of Chemistry and Biomolecular Sciences, Macquarie University, Sydney, Australia

<sup>‡</sup>Department of Analytical Chemistry, Ruhr-University Bochum, Bochum, Germany

<sup>§</sup>Australian Proteome Analysis Facility, Macquarie University, Sydney, Australia

## Supporting Information

**ABSTRACT:** The targeted analysis of proteins in complex biological samples is best achieved using selected reaction monitoring (SRM). To maximize the sensitivity of this approach, sample fractionation or enrichment is still required, particularly to detect less abundant proteins in clinically relevant biofluids. Here, we report the development of multidimensional protein identification technology (MudPIT)-SRM, taking advantage of the robust online strong cation exchange chromatography for tryptic peptide fractionation and combining it with the multiplexed, quantitative attributes of SRM. The classical MudPIT method has been modified with an in-line strategy to introduce reference peptides onto the analytical column to enable quantitation at each salt step. Applying the MudPIT-SRM approach to profile abundant plasma proteins, we demonstrated mean increases in peak areas of almost 90% compared to conventional SRM. MudPIT-SRM analyses of low abundant proteins present in human wound fluid exudates similarly demonstrated increased peak areas and enabled the detection of proteins which were below the lower limit of detection when analyzed by conventional SRM. The MudPIT-SRM method is relatively facile to conduct and offers performance advantages to enhance sensitivity for biomarker studies.



Selected reaction monitoring mass spectrometry (SRM-MS) is a highly selective and sensitive analytical method applied to biomedical and pharmaceutical research. Over the past few years, efforts have grown to implement SRM for proteomics with particular emphasis toward clinical biomarker applications.<sup>1–11</sup> SRM-MS is exceedingly applicable for complex protein mixtures, enabled by highly sensitive analyte detection using consecutive mass analysis steps of defined ions. The selection of defined ions includes the precursor ion and one or more product ions generated by collision induced dissociation (CID). The transition of a selected precursor ion to a product ion provides specificity and high sensitivity detection of a predefined analyte within the complex background common to biological samples. SRM is mainly performed on triple-quadrupole instruments but can also be conducted on Ion-trap instruments.<sup>12,13</sup> The fast ion scanning rates of triple quadrupole instruments facilitate the simultaneous monitoring of multiple analytes. Hence, SRM-MS comprises the advantages of multiplexed, quantitative target analysis within a single run with reliable analyte identification achieved by monitoring multiple transitions for each peptide. These advantages, however, are best exploited with simple protein mixtures or with highly abundant proteins in complex specimens like blood plasma.<sup>14–18</sup>

To detect less abundant proteins by SRM, fractionation strategies are still needed to reduce sample complexity to

overcome ion suppression effects and limit interferences of coeluting peptides. Commonly applied methods involve immunodepletion of the most abundant plasma proteins or by immunoenrichment to purify an analyte.<sup>19,20</sup> Additionally, strong cation/anion exchange chromatography (SCX/SAX) is predominantly used as a robust and facile methodology for charge-based sample fractionation. Interestingly, although online SCX, exemplified in the multidimensional protein identification technology (MudPIT),<sup>21–23</sup> is a widely dispersed, robust method that is routinely applied to discovery-based proteomics, the linking of MudPIT with SRM has not been reported. The MudPIT strategy combines sample purification (desalting), prefractionation, and concentration within a simple chromatographic gradient.<sup>24–26</sup> The reduced sample complexity allows for more optimal usage of the mass spectrometer dynamic range, facilitating sensitivity enhancement.

We anticipate that coupling of online sample fractionation with SRM will overcome crucial peptide losses, especially for low abundant proteins. Many of the losses are associated with the numerous sample manipulation steps associated with offline methods including, sample concentration, buffer exchanges, or resuspension. Here, we describe MudPIT-SRM for the first

Received: October 27, 2011

Accepted: January 5, 2012

Published: January 5, 2012

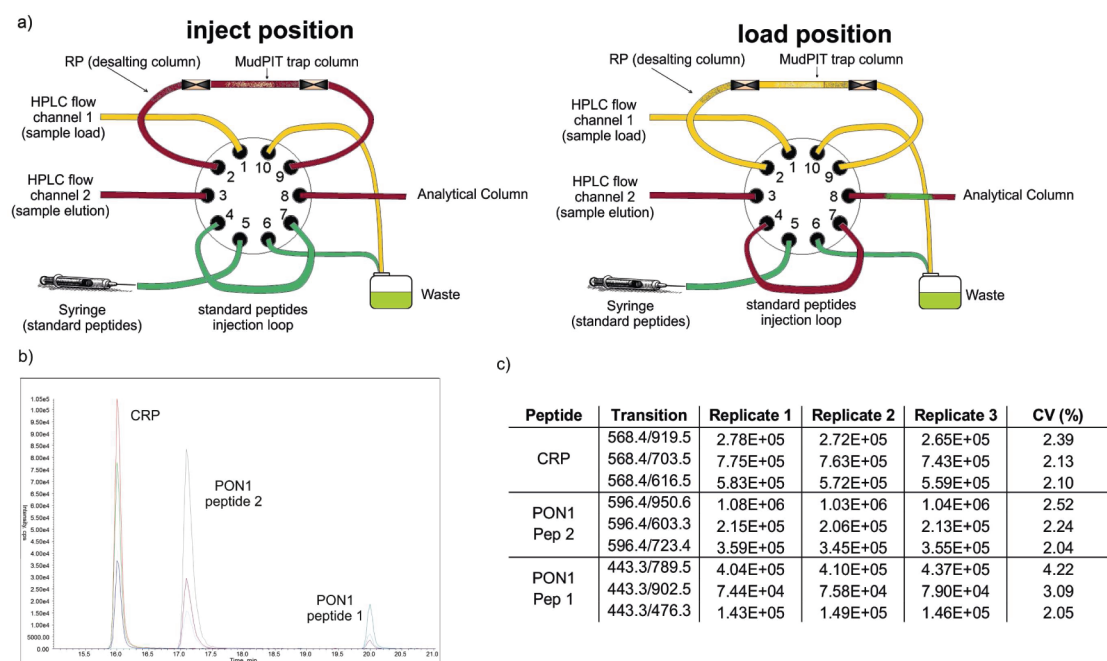


**Figure 1.** (a) Flow scheme of sample injection, sample loading, salt step elution, and reference peptide infusion applied in MudPIT-SRM. (b) Representative elution profile XIC of the reference peptides for CRP and PON1 (three SRMs are used to target each peptide). (c) Proof of reproducible reference peptide injection using continuous peptide infusion into an infusion loop bypassing the trapping column system. Peptides are listed on the basis of their elution order.

time and evaluate performance compared to conventional SRM in terms of sensitivity and quantitation improvements associated with protein biomarker applications. We also describe the introduction of labeled reference peptides via an inline injection loop to facilitate quantitation for MudPIT analyses. Our study demonstrates that MudPIT-SRM is a robust method offering improved capacity to resolve and quantitate candidate biomarkers from biological fluids.

## EXPERIMENTAL SECTION

**Chemicals.** HPLC grade acetonitrile (ACN), methanol, and ammonium acetate ( $\text{NH}_4\text{Ac}$ ) were purchased from Merck (Kilsyth, Australia). Formic acid (FA) and ammonium bicarbonate were obtained from Sigma-Aldrich (Sydney, Australia).

**Sample Collection and Preparation.** Human plasma from a healthy individual was collected in EDTA tubes as previously described.<sup>27</sup> Human wound fluid samples were delivered from the clinic for plastic surgery and serious burn victims at the University hospital “Bergmannsheil” in Bochum, Germany, in a study approved by the Ruhr-University Bochum ethics committee (Ref. No. 2028). Two types of wound fluids were collected; nonhealing wounds from foot ulcers of diabetes mellitus type 2 patients and normal healing burn wounds from otherwise healthy individuals. Fluids were obtained by applying open-pored polyvinyl alcohol (PVA) hydro foam to a wound area to soak excreted material. Soaked foams were removed from the wound, and the retained proteins were obtained after several washes with a Complete protease inhibitor cocktail tablet (Roche, Basel, Switzerland) containing 25 mM ammonium bicarbonate buffer. Samples were immediately frozen in liquid Nitrogen and stored at  $-80^\circ\text{C}$ .

The protein content in plasma and in the wound fluids was estimated by BCA assay kit (BCA Protein Assay Reagent, Pierce, Rockford, Illinois). One milligram of protein was

digested with sequencing grade trypsin (Promega, Alexandria, Australia) at  $37^\circ\text{C}$  in a 1:100 ratio of enzyme to protein in a 30% methanol solution (25 mM  $\text{NH}_4\text{CO}_3$ ; pH 8). Cysteine residues were first reduced with 10 mM dithiothreitol (DTT) at  $37^\circ\text{C}$  for 1 h, followed by alkylation at room temperature using 25 mM iodoacetamide (IAA) for 1 h. Peptides were vacuum concentration and reconstituted to 2.5 mg/mL in 2% ACN and 0.1% FA.

**LC-MS/MS.** Chromatographic separation was performed using a NanoLC 2D System (Eksigent, Dublin, California, USA). Twenty five micrograms of peptides (10  $\mu\text{L}$ ) were injected onto the MudPIT trapping system using the integrated autosampler. The trapping system consists of a self-packed IntegraFrit fused-silica column with 100  $\mu\text{m}$  inner diameter (New Objective, Inc., Woburn, MA, USA) containing 5 cm reversed phase (RP) material (3  $\mu\text{m}$ , 100  $\text{\AA}$ ; Column Engineering Inc., Ontario, CA, USA) followed by a second self-packed IntegraFrit column (100  $\mu\text{m}$  inner diameter) filled with 5 cm strong cation exchange resin (3  $\mu\text{m}$ , 300  $\text{\AA}$ ; PolyLC, Columbia, MD, USA) and 3 cm RP. It was placed in a 10 port valve to achieve optimal loading and elution conditions.

Injected peptides retained and purified on the first RP trap were transferred to the SCX phase using an effective 30 min (plasma) or 10 min (wound fluid) ACN gradient using an 80% ACN and 0.1% FA buffer. Ten microliters of autosampler injections of 15, 30 (300 plasma only), and 1500 mM  $\text{NH}_4\text{Ac}$  (pH 3) was used for sample fractionation based on the binding strength of the analytes on the SCX resin. Released peptides were trapped on the second RP trap. ACN gradients (30 min plasma and 10 min wound fluids), following each salt injection, enabled analytes to be separated on the 15 cm RP column (3  $\mu\text{m}$ , 100  $\text{\AA}$ ; SGE Analytical Science, Rowville, Victoria, Australia) in-line with the trapping system. In a second injection loop, stable isotope labeled reference peptides were continuously infused using a Harvard model 22 syringe pump

**Table 1.** List of MudPIT and RP-SRM Targeted Peptides in Human Plasma Including Precursor and Product Ion Masses, Mean Peak Area, and Peptide CVs MudPIT Analyzed Plasma Sample

protein	peptide sequence	precursor mass ( <i>m/z</i> )	product ion mass ( <i>m/z</i> )	mean peak area (counts) MudPIT-SRM	mean peak area (counts) RP-SRM	peak area increase (%) MudPIT vs RP-SRM	MudPIT-SRM CV (%)
A1AG2	TEDTIFLR	497.8	764.4	$1.60 \times 10^6$	$1.10 \times 10^5$	93.09	11.81
A1AT	LSITGYDLK	556.0	797.4	$3.43 \times 10^6$	$1.55 \times 10^5$	95.48	5.34
A2MG	QTVSWAVTPK	558.8	788.4	$2.70 \times 10^5$	$7.25 \times 10^4$	73.18	4.62
AACT	ADLSGITGAR	480.8	574.3	$1.35 \times 10^6$	$2.49 \times 10^5$	81.47	6.85
AMBP	ETLLQDFR	511.3	565.3	$2.85 \times 10^5$	$1.86 \times 10^4$	93.47	2.76
ANGT	SLDFTELDVAAEK	719.3	975.5	$2.82 \times 10^5$	$2.28 \times 10^4$	88.63	5.78
	VLSALQAVQGLLVAAQGR	862.0	1111.7	$2.54 \times 10^5$	$1.41 \times 10^4$	95.02	2.09
	ALQDQLVLAALK	634.9	956.6	$2.01 \times 10^5$	$4.51 \times 10^4$	82.24	0.63
APOA1	QGLLPVLESFK	615.8	819.5	$3.22 \times 10^7$	$2.37 \times 10^4$	72.45	6.96
	DYVSQFEGSALGK	700.8	1023.5	$1.32 \times 10^7$	$3.90 \times 10^6$	87.90	4.86
	VSFSALEEYTK	694.3	940.5	$1.04 \times 10^7$	$1.01 \times 10^6$	90.32	8.14
APOB	GFEPTEALFGK	655.0	975.6	$4.57 \times 10^5$	$1.04 \times 10^6$	92.13	3.46
APOC3	DALSSVQESQVAQQAR	859.0	1144.6	$9.54 \times 10^5$	$3.04 \times 10^4$	93.35	7.95
CO3	IHWESASLLR	606.3	695.3	$2.08 \times 10^5$	$1.80 \times 10^5$	81.10	5.62
	TELRPGETLNVNFFLR	624.8	875.5	$1.15 \times 10^6$	$3.75 \times 10^4$	82.01	9.23
	SLSVPPYVIVPLK	701.6	928.6	$2.17 \times 10^6$	$1.10 \times 10^5$	90.44	6.14
CO4A	LELSVDGAK	466.3	689.4	$2.51 \times 10^5$	$1.46 \times 10^5$	93.26	3.11
	VGDTLNLLNR	557.8	629.4	$1.93 \times 10^6$	$8.10 \times 10^3$	96.77	8.21
FIBA	GLIDEVNDQFTNR	761.3	894.4	$1.25 \times 10^7$	$1.15 \times 10^5$	94.06	1.34
FIBB	DNENNVNEYSSELEK	885.1	1197.6	$4.78 \times 10^6$	$1.31 \times 10^6$	89.53	3.73
FIBG	LDGSVDFK	440.7	652.3	$8.48 \times 10^5$	$5.08 \times 10^4$	98.94	10.79
HEMO	GGYTLVSGYPK	571.5	650.4	$1.26 \times 10^6$	$8.20 \times 10^4$	90.34	2.26
HPT $\alpha$	TEGDGVYTLNDK	656.3	1081.5	$1.90 \times 10^5$	$1.66 \times 10^5$	86.86	1.93
HPT $\beta$	VTSIQDWVQK	602.3	1003.5	$2.47 \times 10^6$	$2.59 \times 10^4$	86.34	6.54
KNG1	YFIDFVAR	515.8	720.4	$5.61 \times 10^5$	$2.58 \times 10^5$	89.57	2.33
	DIPTNSPELEETLTHITTK	714.1	813.5	$1.15 \times 10^5$	$4.11 \times 10^4$	92.67	7.04
SAA	SFFSFLGEAFDGR	776.0	822.4	$4.51 \times 10^4$	$5.66 \times 10^3$	95.06	4.19
THRB	ELLESYIDGR	597.8	710.3	$1.48 \times 10^5$	$9.08 \times 10^2$	97.99	9.89
TRFE	EGYGYTGAFR	642.8	771.4	$4.78 \times 10^6$	$7.10 \times 10^3$	95.22	2.77
TTHY	GSPAINVAHVFR	683.9	941.5	$5.12 \times 10^5$	$5.04 \times 10^5$	89.45	4.46
VTDB	VPTADLEDVPLAEDITNILSK	1183.7	1313.7	$7.92 \times 10^5$	$1.27 \times 10^5$	75.11	9.23
VTNC	FEDGVLDPDYPR	711.8	875.4	$2.37 \times 10^5$	$6.42 \times 10^4$	91.89	2.89
mean						$89.22 \pm 5.26$	$5.40 \pm 2.44$

(Harvard Apparatus, Holliston, MA, USA). Reference peptides (300 fmol) were directly transferred to the analytical column using the HPLC.

Eluting ions were transferred to the 4000 QTRAP mass spectrometer (AB SCIEX, Foster City, California, USA) using a 2.4 kV spray voltage and a heating plate temperature of 150 °C. Precursor ions were isolated in quadrupole 1 (Q1), fragmented with collision induced dissociation (CID) in Q2 by collision with nitrogen gas, and their characteristic product ions were detected in Q3, allowing a dwell time for each transition of 20 ms generating a cycle time of 2–3 s, depending on the number of transitions. In nonquantitative investigations, eluting target analytes were validated using SRM triggered MS/MS scans from isolated precursor ions. The MS/MS spectra were searched against the human Swiss-Prot database using the Mascot algorithm with 1.2 Da mass tolerances for precursor and 0.6 for product ions.

**Data Analysis.** For each transition, extracted ion chromatograms (XIC) were generated and the area under the curve (AUC) was determined using the imbedded quantitation tool in the instrument software Analyst (AB SCIEX, Foster City, California, USA). This tool implements the IntelliQuant algorithm. Peak integration was performed using a 3 point

peak smoothing. Within triplicate analyses, retention time shifts of less than 30 s were accepted as reproducible target retention.

## RESULTS AND DISCUSSION

**Flow Path Configuration for MudPIT-SRM.** A 2D LC system with integrated autosampler has been used to achieve optimal performance, reproducibility, and maximized instrument usage time. The flow path configuration shown in Figure 1a allows high flow ( $\mu\text{L}/\text{min}$ ) sample loading (channel 1) and nanoflow ( $\text{nL}/\text{min}$ ) elution on channel 2. In the loading position, the analyte is transferred to the MudPIT trapping system, which consists of a short RP column for online sample desalting followed by an independent SCX/RP hybrid column used for SCX sample fractionation, consistent with the classical MudPIT configuration.<sup>27–29</sup> Briefly, retained peptides on the first RP phase are eluted onto the SCX phase after salts have been washed away by switching the 10-port valve to the inject position and starting the ACN elution gradient. Eluting peptides will bind to the SCX material based on their cationic strength. Injection of buffer with increasing  $\text{NH}_4\text{Ac}$  concentration through the autosampler and 10-port valve in a manner similar the sample injection allows peptides to be eluted. The stronger the peptide cationic strength, the higher is the salt concentration required to elute peptides from the SCX

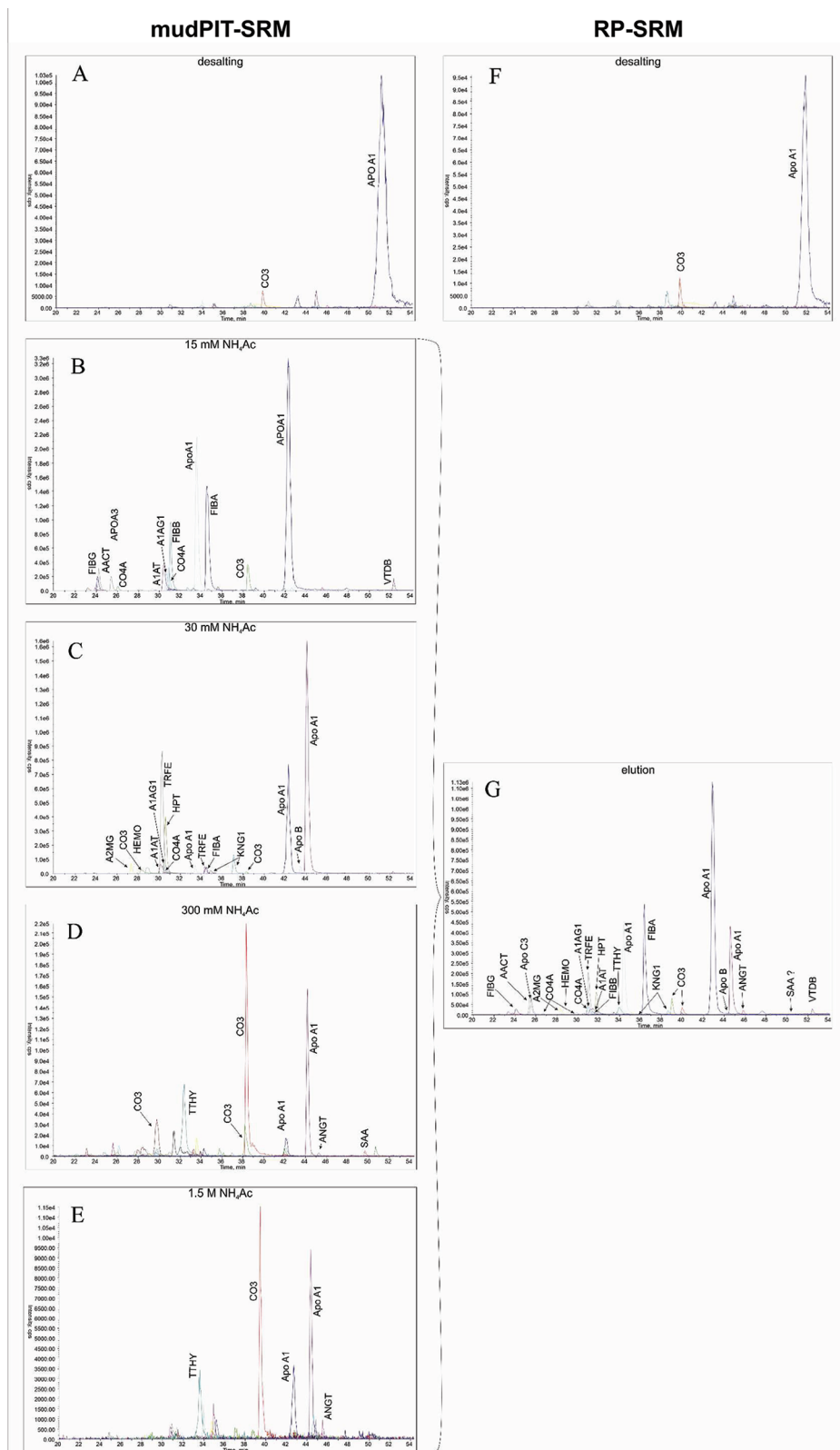


**Figure 2.** LC-SRM analysis targeted the detection of 32 peptides using MudPIT-SRM (Panels A-E) or RP-SRM (Panels F,G). Tryptic peptides from human plasma were separated using 30 min LC gradients and detected by MudPIT-SRM. (A) Desalting, (B) 15 mM  $\text{NH}_4\text{Ac}$  elution, (C) 30 mM  $\text{NH}_4\text{Ac}$  elution, (D) 300 mM  $\text{NH}_4\text{Ac}$  elution, and (E) 1.5 M  $\text{NH}_4\text{Ac}$  elution. For RP-SRM, peptides were (F) desalted or (G) eluted with 1.5 M  $\text{NH}_4\text{Ac}$ .

material. The whole process only depends on autosampler directed sample/salt injections and valve switching, thereby avoiding all offline sample handling after tryptic digestion.

During the entire analysis, three stable isotope labeled reference peptides (C-reactive protein (CRP); ESDTSYVSLK, labeled amino acid underlined, and serum paraoxonase/arylesterase 1

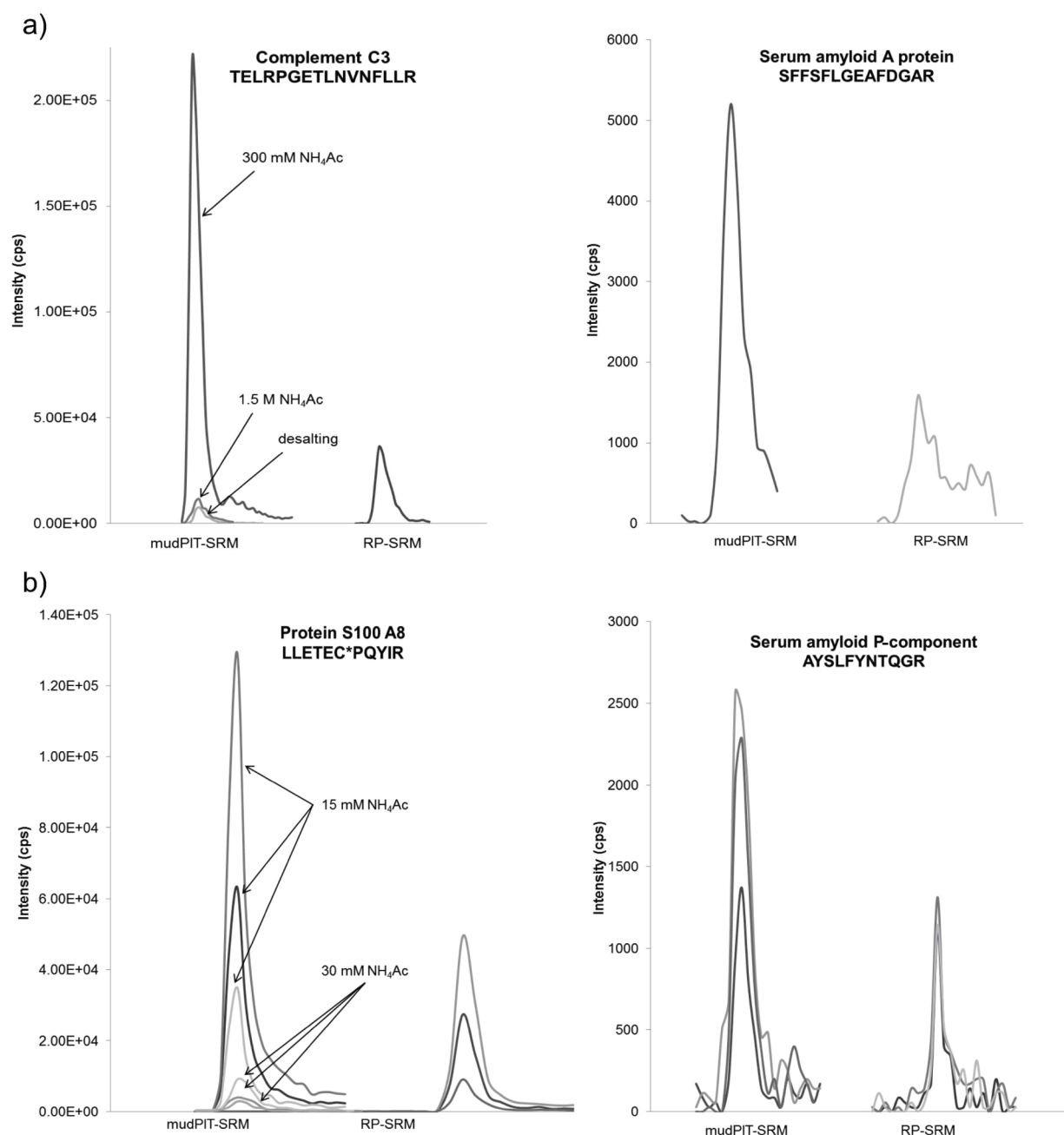


**Figure 3.** MudPIT-SRM induced peak height increases of (a) complement C3 peptide TELRPGETLNVNFLLR and serum amyloid A protein peptide SFFSFLGEAFDGAR in human blood plasma and (b) protein S100 peptide LLETEC\*PQYIR (\* indicates a carbamidomethylation) and serum amyloid P-component targeted in human wound fluids.

(PON1); peptide 1: YVYIAELLAHK; peptide 2: IQNIL-TEEPK) are continuously infused into an injection loop using a syringe pump (placed between valve ports 4 and 7) while the valve is in the inject position. The reference peptides are transferred to the analytical column when a sample is loaded or fractionated by salt injection. Reference peptides, whose representative XICs are shown in Figure 1b, are retained on the analytical column prior to target peptide analyte binding but are eluted collectively with the target peptides, facilitating relative quantitation within and between sample analyses. Reproducible injection of the reference peptides is shown in Figure 1c.

The described chromatography setup improves sample preparation related issues such as sample losses due to

concentration and resuspension after offline SCX fractionation. Further, offline fractionation strategies are time-consuming and increase the preanalysis sample preparation complexity. MudPIT-SRM combines online desalting (cleanup step) and rapid online SCX fractionation with targeted quantitative mass spectrometry to facilitate SRM investigations toward clinical applications in high complex biological material. As MudPIT-SRM takes advantage of sequential salt fractionation steps, analysis time is dictated by the degree of sample fractionation required. For example, a MudPIT-SRM workflow using five step (1 desalting and 4 salt steps) analysis takes approximately five times longer than conventional RP-SRM.

**MudPIT-SRM Applied to Human Plasma.** To demonstrate the utility of MudPIT-SRM, we compared it with

Table 2. Comparison of RP-SRM and MudPIT-SRM Performance in Identifying and Quantifying Targeted Peptides in Human Wound Fluids<sup>a</sup>

protein	peptide sequence	precursor mass ( <i>m/z</i> )	product ion mass ( <i>m/z</i> )	MudPIT-SRM	RP-SRM	peak area changes (%)
ANXA1	GLGTDEDLTLEILASR	851.9	1015.6	d		n/a
			688.4			
			801.5			
ANXA2	SLYYIQDQTK	711.3	895.4	d	d	n/a
			732.4			
			619.3			
ANXA3	GAGTNEDALIEILTTR	837.4	732.4	q	d	n/a
			845.5			
			958.6			
	GIGTDEFTLNR	611.8	1052.5	q	d	n/a
			894.4			
			995.5			
GDRI1	AEEYEFLLTPVEEAPK	876.4	769.4	q		n/a
			870.5			
			1130.6			
			812.4			
GDRI2	TLLGDGPVVTDPK	656.4	755.4			n/a
			927.5			
			973.5			
			787.4			
MMP2	AFQVWSDVTPLR	709.8	1200.6	q	q	-30.3
MMP8	YYAFDLIAQR	630.3	933.5	q	q	24.5
			1096.6			
			862.5			
	DAFELWSVASPLIFTR	926.5	1090.6	q	q	9.8
			833.4			
			904.5			
	ISQGEADINIAFYQR	862.9	911.5	q	q	66.8
			1139.7			
			797.4			
MMP9	QLSLPETGELDSATLK	851.4	1034.5	q		n/a
			933.5			
			734.4			
	AFALWSAVTPLTFTRI	841.0	1092.6	q	q	28.3
			934.5			
			744.4			
	LGLGADVAQVTGALR	720.9	815.5	d	d	n/a
			1029.6			
			871.5			
PROF1	TFVNITPAEVLVVGK	822.5	968.6	q	q	60.5
			1069.6			
			887.5			
	SSFYVNGLTLGGQK	735.9	986.6	q	q	55.3
			773.4			
			1006.5			
	STGGAPTFFNVTVTK	690.4	909.5	q	q	36.9
			503.8			
			708.4			
SAMP	VGEYSLYIGR	578.8	957.5	q	d	n/a
			871.5			
			1000.5			
	AYSLFSYNTQGR	703.8	825.4	q	d	n/a
			972.5			
			738.4			
S100A4	ELPSFLGK	445.7	551.3	d		n/a
			464.3			
			648.3			
	ALDVMVSTFHK	624.3	849.4	d	d	n/a
			948.5			
			718.4			

Table 2. continued

protein	peptide sequence	precursor mass ( <i>m/z</i> )	product ion mass ( <i>m/z</i> )	MudPIT-SRM	RP-SRM	peak area changes (%)
S100A7	GTNYLADVFEK	628.8	708.4	q	q	-21.2
			821.4			
			984.5			
S100A8	LLETEC*PQYIR	711.4	965.4	q	q	49.7
			1066.5			
			1196.5			
S100A11	C*IESLIAVFQK	654.4	1034.6	q		n/a
			818.5			
			905.5			
S100A12	GHFDTLK	452.7	710.4	d	q	n/a
			563.3			
			448.3			
S100P	YSGSEGSTQTLTK	679.8	835.4	q		n/a
			1108.5			
	ELPGFLQSGK	538.3	964.5	q	q	-63.2
			417.2			
			833.4			
			736.4			

<sup>a</sup>Abbreviations used in the table refer to n/a = not applicable, d = detectable, q = quantifiable, and \* = carbamidomethylation.

conventional SRM using RP peptide separation using human plasma. The plasma was immunodepleted of albumin and immunoglobulin gamma, and 32 peptides from 24 highly abundant plasma proteins were monitored (Table 1). These assays of clinical utility were selected on the basis of previous observations of analytical performance that showed high quantitative reproducibility using nanoflow LCMS and a 4000 QTRAP with a cohort of cancer patients.<sup>30</sup> To maintain similar reproducibility, the current study utilized RP-SRM with the MudPIT trapping system still in line using a single high concentration salt elution step. Therefore, the trapping column loading capacity and the peptide retention times remained constant. A sequential 5 step MudPIT-SRM fractionation using 0, 15, 30, 300, and 1500 mM NH<sub>4</sub>Ac was carried out to achieve optimal separation without sacrificing excessive analysis time. An effective organic elution gradient of 30 min follows each salt fractionation step. Including sample loading and column re-equilibration, the total analysis time is 7 h per sample.

MudPIT-SRM and RP-SRM detection was compared using peak intensity and peak area of targeted peptide transitions (Table 1). Elution profiles of MudPIT-SRM and RP-SRM analysis (Figure 2) demonstrate improvements in overall peak intensity and mean peak area for all target peptides using MudPIT-SRM. Figure 3 depicts examples of intensity increases associated with MudPIT-SRM for complement C3 (CO3) peptide TELRPGETLNVNFLLR and the serum amyloid A4 (SAA) peptide SFFSFLGEAFD GAR. From Figure 2, it is evident that peptides analyzed with MudPIT-SRM showed an intensity increase of at least 50% compared to conventional RP-SRM. Determination of AUC for MudPIT- and RP-SRM (Table 1) further demonstrates the sensitivity enhancement of MudPIT-SRM as mean peak area increases to  $89.2 \pm 5.3\%$  (range of 73–98%) and, therefore, represents almost an order of magnitude improvement to support improved quantitation limits. As a consequence of salt step elution methodology, occasionally, some peptides were spread across more than one fraction with a high intense peak in one salt fraction and a more minor component in the next fraction.

However, as long as those peptides are above the lower limit of quantitation (LLOQ), which we defined as 10 times the

noise, the peak areas are able to be accurately summed. Triplicate MudPIT-SRM analyses of a human plasma sample reveal excellent reproducibility with mean coefficients of variation (CV) of  $5.40 \pm 2.44\%$ , ranging between 0.6 and 11% (Table 1), which is comparable to CVs reported from RP-SRM studies.<sup>11,27,28</sup>

Despite the differences of MudPIT- and RP-SRM in the elution conditions, the two strategies show similarity in the desalting step. The presence of an APOA1 and a CO3 peptide in the desalting step of both SRM methods is most likely contributed to a limitation in binding capacity of peptides on the SCX material due to the high abundance of these plasma proteins. Although 5–10% of these peptides were not retained on the SCX phase, these peptides were still detected and can be used for quantitation.

The multiple salt step elution increases peptide purity and reduces the complexity within each elution step improving known electrospray ionization (ESI) issues such as ion suppression caused by coelution of analytes. To visualize the changes in ion suppression, a setup described by Jessome and Volmer<sup>29</sup> has been assessed. Briefly, a mixture of the three isotope labeled peptides (500 fmol/ $\mu$ L) was continuously infused (3  $\mu$ L/h) after the analytical column infused into the flow path of an elution gradient. Performing a SRM experiment targeting the three peptides allows for continuous monitoring of the ionization efficiency. Triplicate analyses of (1) the background without a complex solution, (2) RP-SRM separation of human plasma, and (3) MudPIT-SRM separation of human plasma have been accomplished (Figure S-1, Supporting Information). Interestingly, this experiment revealed changes in ionization efficiency throughout the entire gradient, not merely when high amounts of peptides are coeluting. Monitored background demonstrates reproducible ionization efficiency of infused peptides within the triplicate analyses (Figure S-2, Supporting Information). However, both RP-SRM and MudPIT-SRM showed increased intensities of CRP and PON1 peptide 2 in the desalting step compared to the background, which is consistent with improved ionization in this step. RP-SRM elution of the plasma sample following the desalting step results in a significant reduction of targeted

peptide transition intensities by 70–80%, demonstrating a high degree of ion suppression. Under the same experimental conditions, the MudPIT-SRM strategy showed higher ion counts per second for the desalting step compared to RP-SRM, which further increased in the 15 mM (10–20% CRP and PON1 peptide 2; 60% PON1 peptide 1) and 30 mM (50–60% CRP and PON1 peptide 2; 230% PON1 peptide 1) salt injection steps before the intensities decreased to comparable levels as in the RP-SRM elution step when performing the 1.5 M salt elution. Although PON1 peptide 1 showed slightly different behavior in the ion suppression experiment, which is most likely related to the 3+ charge state, it followed the overall trend of the other two peptides.

**Targeting Less Concentrated Proteins in Human Wound Exudates.** The MudPIT-SRM method has shown significant improvements in SRM performance for targeting highly concentrated plasma proteins; however, a chief purpose of the online SCX fractionation strategy is not only to increase quantitation accuracy of highly concentrated proteins but also to enable the detection and quantitation of less abundant proteins (lower ng/mL). Additionally, this strategy should contribute to rapid sample analysis especially for SRM-MS demands in clinical applications where time can be a key factor. In order to demonstrate the application of MudPIT-SRM in this situation, candidate biomarkers from human wound fluids, which were previously identified in a discovery experiment comparing fluids of nonhealing wounds to normal healing wounds from burn victims (manuscript in preparation), have been analyzed.

A selection of potential discriminating biomarkers that are commonly known to be of ng/mL concentration in plasma (e.g., metalloproteinases, S100 proteins) were chosen (Table 2) and analyzed with MudPIT-SRM using 79 transitions optimized for SCX elution (Table 2). Corresponding MS/MS spectra of targeted peptides are shown in Figure S-3, Supporting Information. In a first instance, peptide elution gradients were optimized to achieve actual gradient times of just 10 min. Further improvements might be possible using faster scanning instruments, since the 10 min gradient is not limited by the chromatographic separation but the detection of eluting ions by the MS. Cycle times of 2 s, generated by 20 ms dwell time, only allow a reduction of the actual gradient time to 10 min. Further gradient reduction would lead to peak width smaller than 12 s, causing irreproducibility due to inaccurate data acquisition. Assessment of MudPIT using the highly abundant plasma proteins (Table 1) showed elution of the same peptides in the 300 mM and 1.5 M NH<sub>4</sub>Ac steps; hence, the 300 mM salt step was removed to optimize reproducibility and shorten the run. Targeted peptides of low abundant proteins from a nonhealing wound exudate were analyzed using the MudPIT-SRM strategy and compared to a RP-SRM analysis of the same sample.

Triplicate analyses readily demonstrated the advantage of MudPIT-SRM for detection of less abundant proteins, with peak area increases of 25–60% (Table 2). Further, the MudPIT-SRM strategy enabled peptides, which were below the LLOQ in the RP-SRM approach, to be quantitated. For example, two different serum amyloid P (SAMP) peptides, VGEYSLYIGR and AYSLFSYNTQGR, and two Annexin A3 (ANXA3) peptides, GAGTNEDALIEILTTR and GIGT-DEFTLNR, Rho GDP-dissociation inhibitor (GDIR) 1 (AEEYEFLTPVEEAPK), S100 P peptide YSGSEGSTQTLTK, S100 A11 (C\*IESLIAVF, where \* indicates a carbamidome-

thylation of cysteine residues), and the matrix metalloproteinase 9 (MMP9) peptide QLSPETGELDSATLK were below the lower limit of detection (LLOD) in conventional RP-SRM but were quantifiable with MudPIT-SRM. Additionally, the MudPIT-SRM strategy enabled peptides of ANXA1 (GLGTDEDTLIEILASR) and S100 A4 (ELPSFLGK) to be detected. These two peptides were below the LLOD using RP-SRM. However, no improvements were observed for MMP9 peptide LGLGADVAQVTGALR and one S100 A4 peptide (ALDVMVSTFHK). These peptides remained below the LLOQ in both chromatographic configurations. Paradoxically, S100P (ELPGFLQSGK), the S100 A7 peptide GTNYLADVFEK, and MMP2 (AFQVWSDVTPLR) revealed significantly greater peak areas in the RP-SRM strategy. Four of the S100 peptides studied here have previously been analyzed by SRM in the serum of rheumatoid arthritis patients. In their report, Liao et al.<sup>31</sup> used 1 mL of serum, affinity depletion of abundant proteins, and extensive size exclusion fractionation prior to SRM. In the current study, we were able to detect each of these peptides using the MudPIT-SRM configuration following injection of small volumes of unfractionated wound fluid. Comparisons of the quantitative characteristics of these two approaches are difficult to make given differences in samples, sample preparation strategies, and improvements in mass spectrometry hardware.

For more than 90% of the targeted low abundant proteins, it was clearly advantageous to apply MudPIT-SRM over RP-SRM, allowing peptides to be quantified or detected which were previously refractory to analyses. Even though MudPIT-SRM requires longer analysis time compared to RP-SRM, it is the gains made through sample fractionation that leads to detection of less abundant analytes. We have shown here that gradient elution times can be substantially reduced, akin to the time normally used for RP-SRM, yet tremendous gains in sensitivity make this approach highly attractive for detection of proteins that are at low levels or masked in unfractionated samples applied to RP-SRM analysis.

## ■ CONCLUSION

We have described the integration of the widely used MudPIT approach with SRM and demonstrated its performance advantages over conventional RP-SRM. MudPIT-SRM reduces ion-suppression, improves signal by as much as 1 order of magnitude, and is compatible with rapid chromatography for analysis of biological fluids. These attributes identify MudPIT-SRM as a useful method for protein biomarker studies, particularly suited for the analysis of clinically relevant biological fluids. One drawback of the MudPIT-SRM approach is the additional time required to complete the analysis using multiple salt fractionation steps compared with conventional RP-SRM. Nonetheless, the superior signal gain achieved with MudPIT-SRM (~90%) may overcome this attribute for analyses of biologically relevant proteins that may otherwise evade detection using conventional SRM approaches.

## ■ ASSOCIATED CONTENT

### 📄 Supporting Information

Ionization efficiency experiments performed on the 4000 QTRAP; real time plots of monitored ion suppression; acquired SRM-triggered peptide MSMS spectra of targeted proteins in human wound fluids. This material is available free of charge via the Internet at <http://pubs.acs.org>.

## ■ AUTHOR INFORMATION

## Corresponding Author

\*Address: APAF, Macquarie University, Sydney, Australia, 2109. Tel: +612 9850 6218. Fax: +612 9850 6200. E-mail: mmolloy@proteome.org.au.

## ■ ACKNOWLEDGMENTS

C.K. is the recipient of a Macquarie University cotutelle PhD scholarship. M.P.M. is the recipient of an NHMRC Career Development Award. Aspects of this research were conducted at APAF, supported by the Australian Government's NCRIS/EIF programs.

## ■ REFERENCES

- (1) Anderson, N. L.; Anderson, N. G.; Pearson, T. W.; Borchers, C. H.; Paulovich, A. G.; Patterson, S. D.; Gillette, M.; Aebersold, R.; Carr, S. A. *Mol. Cell. Proteomics* **2009**, *8*, 883–886.
- (2) Lange, V.; Picotti, P.; Domon, B.; Aebersold, R. *Mol. Syst. Biol.* **2008**, *4*, 222.
- (3) McIntosh, M.; Fitzgibbon, M. *Nat. Biotechnol.* **2009**, *27*, 622–623.
- (4) Rodriguez, H.; Rivers, R.; Kinsinger, C.; Mesri, M.; Hiltke, T.; Rahbar, A.; Boja, E. *Proteomics Clin. Appl.* **2010**, *4*, 904–914.
- (5) Schiess, R.; Wollscheid, B.; Aebersold, R. *Mol. Oncol.* **2009**, *3*, 33–44.
- (6) Wang, P.; Whiteaker, J. R.; Paulovich, A. G. *Cancer Biol. Ther.* **2009**, *8*, 1083–1094.
- (7) Chiu, C.-L.; Randall, S.; Molloy, M. P. *Bioanalysis* **2009**, *1*, 847–855.
- (8) Fortin, T.; Salvador, A.; Charrier, J. P.; Lenz, C.; Bettsworth, F.; Lacoux, X.; Choquet-Kastylevsky, G.; Lemoine, J. *Anal. Chem.* **2009**, *81*, 9343–9352.
- (9) Gallien, S.; Duriez, E.; Domon, B. *J. Mass Spectrom.* **2011**, *46*, 298–312.
- (10) Kitteringham, N. R.; Jenkins, R. E.; Lane, C. S.; Elliott, V. L.; Park, B. K. *J. Chromatogr., B* **2009**, *877*, 1229–1239.
- (11) Addona, T. A.; Abbatiello, S. E.; Schilling, B.; Skates, S. J.; Mani, D. R.; Bunk, D. M.; Spiegelman, C. H.; Zimmerman, L. J.; Ham, A.-J. L.; Keshishian, H.; Hall, S. C.; Allen, S.; Blackman, R. K.; Borchers, C. H.; Buck, C.; Cardasis, H. L.; Cusack, M. P.; Dodder, N. G.; Gibson, B. W.; Held, J. M.; Hiltke, T.; Jackson, A.; Johansen, E. B.; Kinsinger, C. R.; Li, J.; Mesri, M.; Neubert, T. A.; Niles, R. K.; Pulsipher, T. C.; Ransohoff, D.; Rodriguez, H.; Rudnick, P. A.; Smith, D.; Tabb, D. L.; Tegeler, T. J.; Variyath, A. M.; Vega-Montoto, L. J.; Wahlander, A.; Waldemarson, S.; Wang, M.; Whiteaker, J. R.; Zhao, L.; Anderson, N. L.; Fisher, S. J.; Liebler, D. C.; Paulovich, A. G.; Regnier, F. E.; Tempst, P.; Carr, S. A. *Nat. Biotechnol.* **2009**, *27*, 633–641.
- (12) Han, B.; Higgs, R. E. *Briefings Funct. Genomics Proteomics* **2008**, *7*, 340–354.
- (13) Prakash, A.; Tomazela, D. M.; Frewen, B.; MacLean, B.; Merrihew, G.; Peterman, S.; MacCoss, M. J. *J. Proteome Res.* **2009**, *8*, 2733–2739.
- (14) Agger, S. A.; Marney, L. C.; Hoofnagle, A. N. *Clin. Chem.* **2010**, *56*, 1804–1813.
- (15) Barton, C.; Kay, R. G.; Gentzer, W.; Vitzthum, F.; Pleasance, S. *J. Proteome Res.* **2009**, *9*, 333–340.
- (16) Hoofnagle, A. N.; Wu, M.; Gosmanova, A. K.; Becker, J. O.; Wijsman, E. M.; Brunzell, J. D.; Kahn, S. E.; Knopp, R. H.; Lyons, T. J.; Heinecke, J. W. *Arterioscler., Thromb., Vasc. Biol.* **2010**, *30*, 2528–2534.
- (17) Lopez, M. F.; Kuppasamy, R.; Sarracino, D. A.; Prakash, A.; Athanas, M.; Krastins, B.; Rezai, T.; Sutton, J. N.; Peterman, S.; Nicolaidis, K. *J. Proteome Res.* **2010**, *10*, 133–142.
- (18) van Winden, A. W. J.; van den Broek, I.; Gast, M.-C. W.; Engwegen, J. Y. M. N.; Sparidans, R. W.; van Dulken, E. J.; Depla, A. C. T. M.; Cats, A.; Schellens, J. H. M.; Peeters, P. H. M.; Beijnen, J. H.; van Gils, C. H. *J. Proteome Res.* **2010**, *9*, 3781–3788.
- (19) Anderson, N. L.; Anderson, N. G.; Haines, L. R.; Hardie, D. B.; Olafson, R. W.; Pearson, T. W. *J. Proteome Res.* **2004**, *3*, 235–244.
- (20) Anderson, N. L.; Jackson, A.; Smith, D.; Hardie, D.; Borchers, C.; Pearson, T. W. *Mol. Cell. Proteomics* **2009**, *8*, 995–1005.
- (21) Washburn, M. P.; Wolters, D. A.; Yates, J. R. *Nat. Biotechnol.* **2001**, *19*, 242–247.
- (22) Washburn, M. P.; Ulaszek, R. R.; Yates, J. R. *Anal. Chem.* **2003**, *75*, 5054–5061.
- (23) Wolters, D. A.; Washburn, M. P.; Yates, J. R. *3rd Anal. Chem.* **2001**, *73*, S683–S690.
- (24) Keshishian, H.; Addona, T.; Burgess, M.; Mani, D. R.; Shi, X.; Kuhn, E.; Sabatine, M. S.; Gerszten, R. E.; Carr, S. A. *Mol. Cell. Proteomics* **2009**, *8*, 2339–2349.
- (25) Izrael-Tomasevic, A.; Phu, L.; Phung, Q. T.; Lill, J. R.; Arnott, D. *J. Proteome Res.* **2009**, *8*, 3132–3140.
- (26) Addona, T. A.; Shi, X.; Keshishian, H.; Mani, D. R.; Burgess, M.; Gillette, M. A.; Clauser, K. R.; Shen, D.; Lewis, G. D.; Farrell, L. A.; Fifer, M. A.; Sabatine, M. S.; Gerszten, R. E.; Carr, S. A. *Nat. Biotechnol.* **2011**, *29*, 635–643.
- (27) Randall, S. A.; McKay, M. J.; Molloy, M. P. *Proteomics* **2010**, *10*, 2050–2056.
- (28) Prakash, A.; Rezai, T.; Krastins, B.; Sarracino, D.; Athanas, M.; Russo, P.; Ross, M. M.; Zhang, H.; Tian, Y.; Kulasingam, V.; Drabovich, A. P.; Smith, C.; Batruch, I.; Liotta, L.; Petricoin, E.; Diamandis, E. P.; Chan, D. W.; Lopez, M. F. *J. Proteome Res.* **2010**, *9*, 6678–6688.
- (29) Jessome, L. L.; Volmer, D. A. *LCGC North Am.* **2006**, *24*, 498–510.
- (30) McKay, M. J.; Sherman, J.; Laver, M. T.; Baker, M. S.; Clarke, S. J.; Molloy, M. P. *Proteomics Clin. Appl.* **2007**, *1*, 1570–1581.
- (31) Liao, H.; Wu, J.; Kuhn, E.; Chin, W.; Chang, B.; Jones, M. D.; O'Neil, S.; Clauser, K. R.; Karl, J.; Hasler, F.; Roubenoff, R.; Zolg, W.; Guild, B. C. *Arthritis Rheum.* **2004**, *50*, 3792–3803.